



Signature curve for general thin-walled members

Sandor Ádány¹

Abstract

Signature curve is widely used in stability design of cold-formed steel members, since it provides with a simple way to determine critical loads for local, distortional and global buckling, which then can be used in predicting member capacity. Signature curve is created by calculating critical loads by systematically changing the length of the thin-walled member while assuming that the load is uniform along the length and the transverse displacement is one single sine half-wave. Mathematically, these conditions are closely related to the semi-analytical finite strip method, while, practically, correspond to a member with pinned end supports subjected to two concentrated loads at the ends, equal in magnitude but opposite in direction. This definition of signature curve cannot easily be applied to more general cases, however, a possible generalization is presented in the paper. Numerical examples are also shown, by employing the constrained finite element method. If the proposed procedure is applied for basic members, the calculated generalized signature curve exactly coincides with the classic signature curve. It is also shown, however, that meaningful generalized signature curve can be calculated for various loading and supports, or even for members with holes.

1. Introduction

The the most characterizing behavior of cold-formed steel members is buckling, as a direct consequence of their large slenderness. Buckling might occur in various forms, due to longitudinal compressive stresses (e.g., lateral-torsional buckling, local plate buckling, etc.), due to shear stresses (e.g., shear buckling of plates), due to transverse compressive stresses (e.g., web crippling), or due to the combination of various stress components. An important step toward the better understanding the buckling of thin-walled members was the introduction of *signature curve*, which is created by plotting the critical loads as a function of characteristic buckling length, while assuming uniform load along the length (i.e., pure compression or pure bending). The notion of signature curve has been proposed by (Hancock, 1978), who also developed the finite strip method software Thin-Wall (THIN-WALL, 1995) for the easy determination of the signature curve. Later, Schafer proposed the Direct Strength Method, (DSM, 2006) for the design of cold-formed steel members, which requires the knowledge of distortional and local critical loads, proposedly determined by the signature curve of the cross-section. To support the practical application of DSM, he published the CUFSM software (CUFSM, 2006), using the semi-analytical FSM, based on the work of Cheung (1976).

¹ Associate Professor, Budapest University of Technology and Economics, <sadany@epito.bme.hu>

For many of the most widely used cold-formed steel profiles the signature curve has two minimum points, which makes it straightforward to determine the necessary local and distortional critical load values. In other cases the application of DSM is less evident. This initiated the constrained finite strip method, or cFSM, (Adany and Schafer 2006a,b), in which the various buckling types are formally and objectively separated. It is to mention that alternative methods for signature curve determination also exist, most notably the generalized beam theory (GBT), see e.g. Silvestre et al. (2011), Bebiano et al. (2015). Signature curve, typically, is interpreted for pure compression or pure bending, uniform along the member length. This means that longitudinal normal stresses govern the behavior, while other stress components are negligible. In recent years the importance and effect of shear stresses has been studied, see. e.g. Pham and Hancock (2013). FSM for members in (virtually) pure shear has also been proposed, which can produce plots similar to classic signature curves, but for members in pure (or dominant) shear.

In all these works a crucial feature of signature curve determination is that both the analyzed member and the loading (i.e., stresses) are uniform along the member length. That is why semi-analytical FSM can readily and very efficiently be used. In this paper a possible generalization of signature curve is introduced. By utilizing the abilities of the recently proposed constrained finite element method (cFEM), see e.g. Ádány (2017), Ádány et al. (2017), curves similar to signature curves can be defined for virtually any thin-walled member. In this paper, first the semi-analytical FSM, the cFSM and cFEM are briefly summarized, then the notion of *generalized signature curve* is introduced, finally a few examples are presented.

2. FSM, cFSM, cFEM

2.1 Semi-analytical finite strip method

The finite strip method (FSM) can be regarded as a special version of finite element method (FEM) in which special finite elements are used. The most essential feature of FSM is that there are two pre-defined directions, and the base functions (or: interpolation functions) are different in the two directions. In classical semi-analytical FSM used for thin-walled members, as in Cheung (1976), the structural member to be analyzed is discretized only in the transverse direction, while in the longitudinal direction there is no discretization, i.e., in this direction there is only one element (i.e., strip) along the member. In a strip each displacement function is expressed as a product of transverse and longitudinal base functions. In the transverse directions polynomials are used, while in the longitudinal direction trigonometric functions are used, that can be written as follows (with using the notations of Fig. 1).

$$u(x, y) = \left[\left(1 - \frac{y}{b}\right) \quad \left(\frac{y}{b}\right) \right] \begin{bmatrix} u_1 \\ u_2 \end{bmatrix} \cos \frac{m\pi x}{a} \quad (1)$$

$$v(x, y) = \left[\left(1 - \frac{y}{b}\right) \quad \left(\frac{y}{b}\right) \right] \begin{bmatrix} v_1 \\ v_2 \end{bmatrix} \sin \frac{m\pi x}{a} \quad (2)$$

$$w(x, y) = \left[\left(1 - \frac{3y^2}{b^2} + \frac{2y^3}{b^3}\right) \quad \left(-x + \frac{2y^2}{b} - \frac{x^3}{b^2}\right) \quad \left(\frac{3y^2}{b^2} - \frac{2y^3}{b^3}\right) \quad \left(\frac{y^2}{b} - \frac{y^3}{b^2}\right) \right] \begin{bmatrix} w_1 \\ \theta_1 \\ w_2 \\ \theta_2 \end{bmatrix} \sin \frac{m\pi x}{a} \quad (3)$$

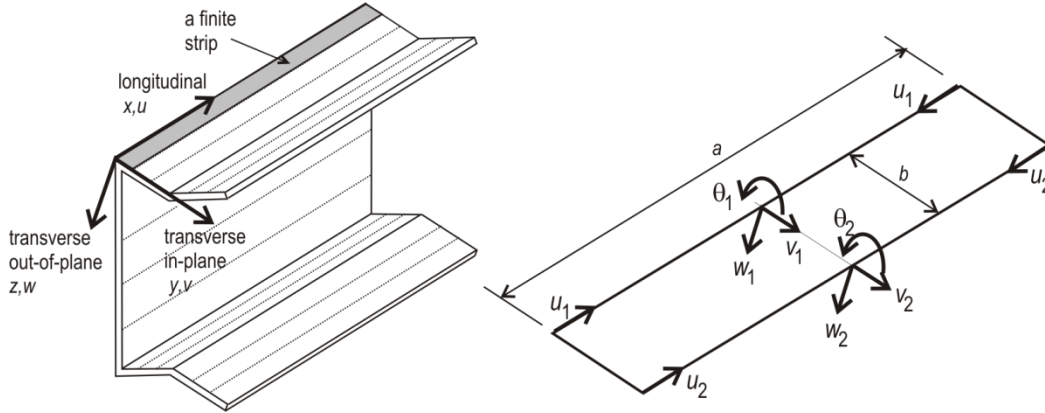


Figure 1: Finite Strip Method discretization and basic terminology

If FSM is applied to solve linear buckling problems to get critical loads and buckling shapes, first the elastic and geometric stiffness matrices must be constructed for a strip, then from the local stiffness matrices the member's (global) stiffness matrices (elastic and geometric, \mathbf{K}_e and \mathbf{K}_g) must be compiled, resulting in the eigen-buckling problem, as follows.

$$\mathbf{K}_e \Phi - \Lambda \mathbf{K}_g \Phi = \mathbf{0} \quad (4)$$

with

$$\Lambda = \text{diag} \langle \lambda_1 \lambda_2 \lambda_3 \dots \lambda_{nDOF} \rangle \quad \text{and} \quad \Phi = [\Phi_1 \Phi_2 \Phi_3 \dots \Phi_{nDOF}] \quad (5)$$

where λ_i is the critical load multiplier and Φ_i is the associated buckling shape, and $nDOF$ denotes the number of degrees of freedom.

2.2 Constrained finite strip method

The constrained FSM (cFSM) is a special version of FSM that uses mechanical criteria to enforce deformations to be consistent with the characteristics of a deformation class, i.e., global (G), distortional (D), local (L), shear (S), or transverse extension (T). The method is originally presented e.g. in Ádány and Schafer (2006a,b), later extended by Ádány and Schafer (2014a,b). Once the mechanical criteria are transformed into constraint matrices, any FSM displacement field \mathbf{d} (including an eigen-buckling mode Φ) may be constrained to any modal \mathbf{d}_M deformation space via:

$$\mathbf{d} = \mathbf{R}_M \mathbf{d}_M \quad (6)$$

where \mathbf{R}_M is a constraint matrix, and M might be G, D, L, S and/or T. When modal decomposition is applied to eigen-buckling solution, Eq (6) must be substituted into Eq (4), which leads to another generalized eigen-value problem, given in the reduced M deformation space, as follows:

$$\mathbf{R}_M^T \mathbf{K}_e \mathbf{R}_M \Phi_M - \Lambda \mathbf{R}_M^T \mathbf{K}_g \mathbf{R}_M \Phi_M = \mathbf{0} \quad (7)$$

The constraint matrices are based on mechanical criteria which characterize the deformation modes. The criteria are expressed mostly by setting certain displacement and displacement

derivatives to zero. For example, G, D and L modes are characterized by zero transverse extension and zero in-plane shear, but L modes furthermore are characterized by zero longitudinal extension. The application of the constraint matrix enforces to fulfil certain relationship between various nodal degrees of freedom. Another view of constraint matrix is that the column vectors of the matrix are the modal base vectors of the displacement field that is represented by the constrain matrix.

It is to emphasize that constraining, or modal decomposition, manipulates the cross-section deformations, but essentially independent of the longitudinal displacements, even though the constraining procedure requires certain criteria to fulfil from the longitudinal shape functions, too. That is why it was straightforward to change the trigonometric shape functions of FSM into polynomial shape functions, which transforms a ‘finite strip’ into a ‘shell finite element’.

2.3 Constrained finite element method

Constrained finite element method (cFEM), see e.g. Ádány (2017a), Ádány et al. (2017), is essentially a shell finite element calculation, similar to cFSM, but the trigonometric longitudinal shape functions are replaced by multiple polynomial shape functions, i.e., a strip is replaced by multiple rectangular shell elements along the length of the member, see Fig. 2. In order to maintain constraining ability, the longitudinal shape functions are carefully selected. The shell element and its nodal degrees of freedom are illustrated in Fig. 3, discussed in detail in Ádány (2016a) and Visy and Ádány (2017).

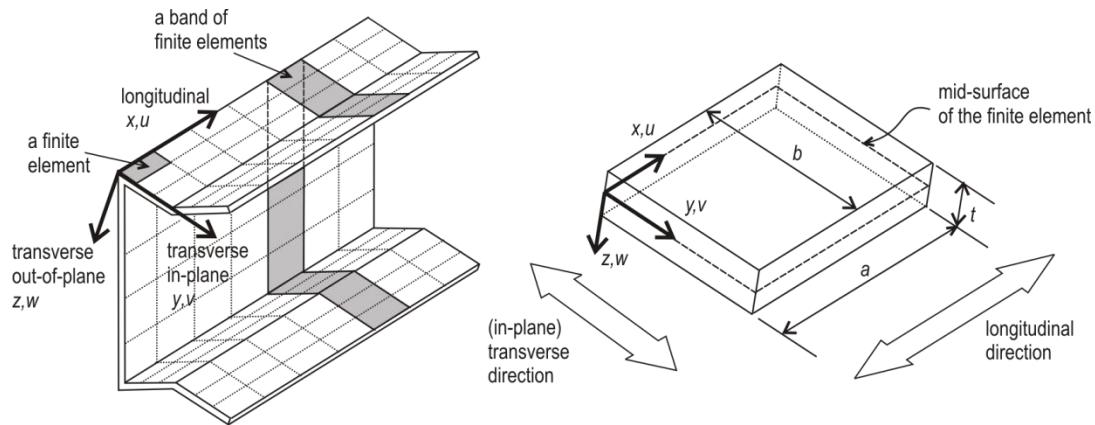


Figure 2: cFEM discretization and basic terminology

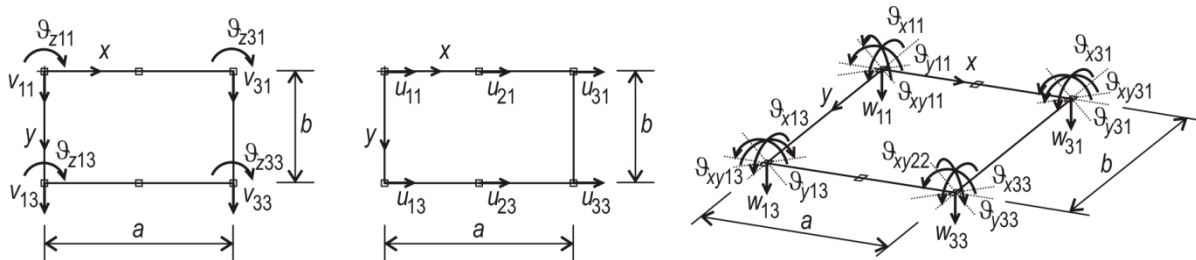


Figure 3: Nodal degrees of freedom for the shell element of cFEM

The shell element can be used as any other shell elements, but can also be constrained, i.e., the solution of the problem can be constrained into a preselected deformation space. When used to buckling problems, therefore, buckling solution (i.e., buckled shapes and associated critical load values) can be calculated to arbitrary thin-walled members which can reasonably be modelled by rectangular shell finite elements. Many examples are presented in earlier papers, e.g., cFEM being applied to shear buckling, (Ádány, 2016b), to purlins (Hoang and Ádány, 2017), to members with holes (Ádány, 2017b), or to members with varying cross-sections (Ádány, 2017c).

All the previously presented cFEM examples are calculated by following the typical FEM approach, namely: the applied longitudinal shape functions are characterized by one single non-zero nodal displacement, while all the other nodal displacements are zero. However, it was also mentioned in Ádány et al (2017), that Fourier-like longitudinal distributions can also be assumed for the longitudinal displacements, as illustrated in Fig. 4. As it is shown in the next Section, this Fourier-like series of longitudinal shape functions can be used to calculate the generalized signature curves.

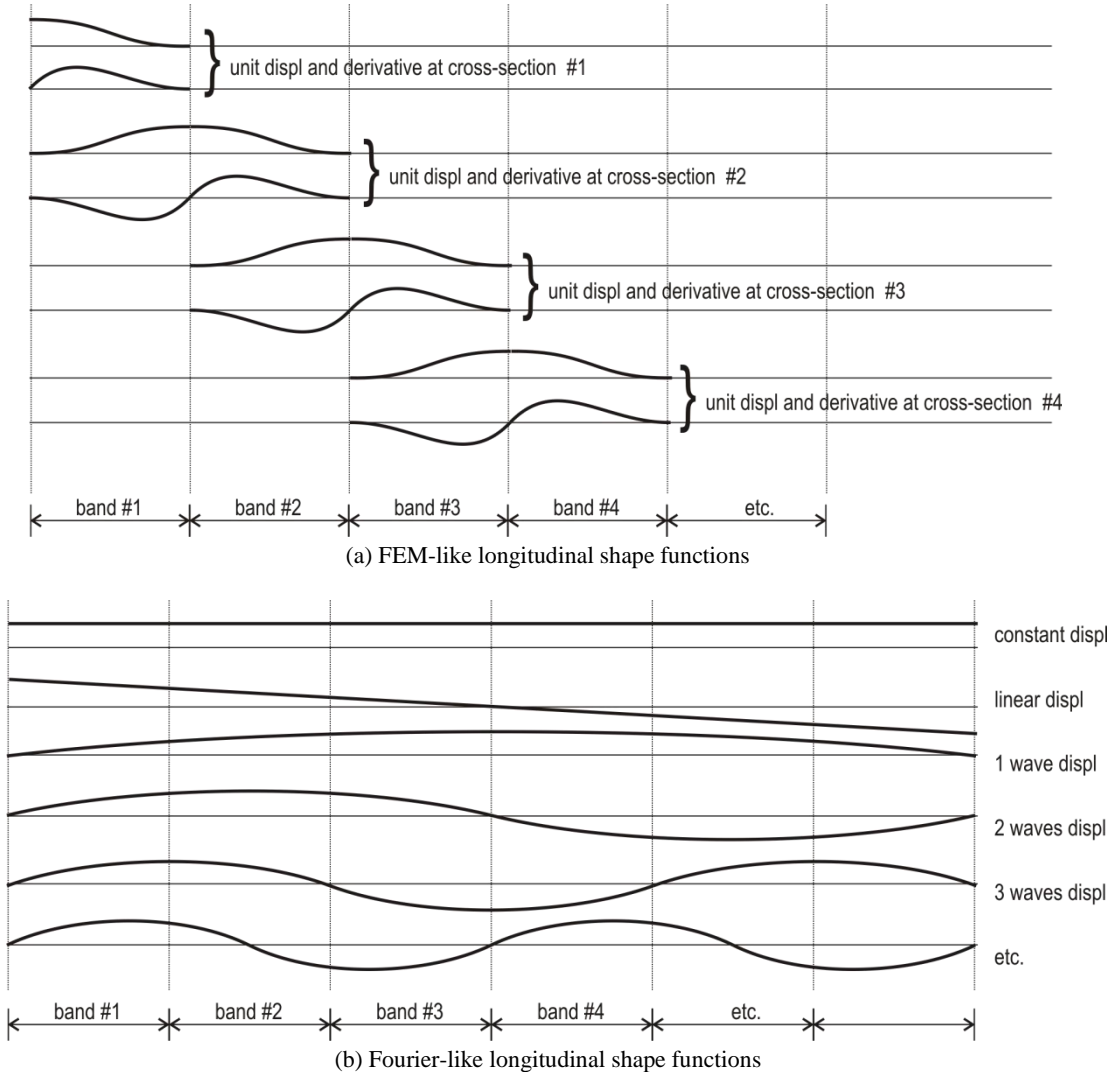


Figure 4: Longitudinal shape functions in cFEM

3. Signature curve and its generalization

Let us consider a prismatic thin-walled member, which is locally and globally hinged at both ends and subjected to uniform loading. If linear elastic buckling analysis is performed, the longitudinal displacements of the buckled shapes are sinusoidal, consisting of one or multiple half-waves. The transverse displacements (i.e., the cross-section displacements) of the buckled shapes are diverse, but it is usual to define deformation classes and interpret the displacements as a combination of displacements from the characteristic classes. The practically most important classes are: global (G), distortional (D), and local (L), but other classes exist, too, namely: shear (S) and transverse extension (T).

In order to get the signature curve, the above buckling problem (i.e., generalized eigen-value problem) must be solved repeatedly by systematically changing the member length, while ensuring that the longitudinal displacements consist of one single half-wave. If the lowest eigen-value (i.e., critical load) is taken for each length, and the critical value is plotted in the function of the (logarithm of) length, this results in the signature curve, see Fig. 5. It is to observe that the shape functions of the semi-analytical FSM identical to those behind the signature curve, therefore FSM is an ideal (and, efficient) tool in determining signature curves.

Almost always the signature curve has minimum points at smaller lengths. These minimum points identify those half-wave lengths at which the given thin-walled member is most susceptible to buckle. In many practical cases there are two minimum points, see Fig. 5, the one with the smaller length is typically associated with local plate buckling while the other one with distortional buckling. These lengths and the associated critical load values are strongly dependent on the cross-section and also on the stress distribution over the cross-section, but the critical values are not too sensitive to the length in the close vicinity of the minimum points. The experience is that these lengths are usually much smaller than practical member lengths. In reality, therefore, L and D buckling occurs with multiple longitudinal waves, but still the minimum points of the signature curve can approximate the distortional and local critical load. If the thin-walled member is long enough, the D and L critical loads are not much affected by the end supports, neither, thus the minimum points of the signature curve can be regarded as reasonable approximations of the D and L critical loads independently of the actual characteristics of the member.

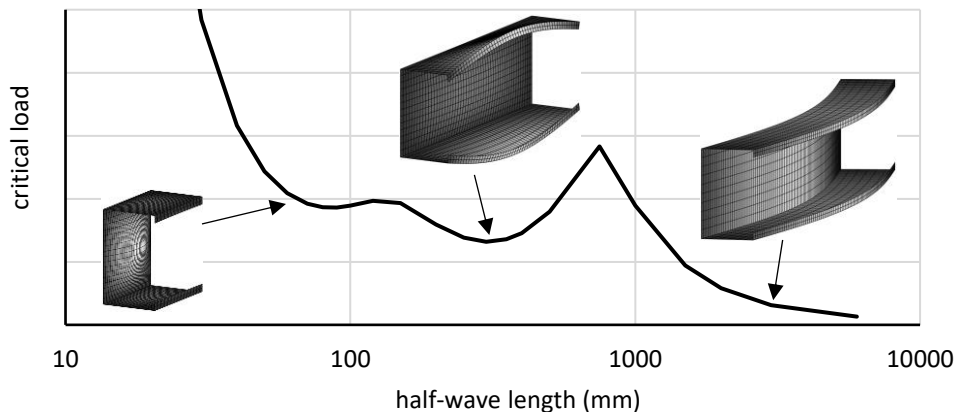


Figure 5: Sample signature curve for a lipped channel

Based on the characteristics and practical application of the signature curve, it can be concluded that the notion of signature curve belongs rather to the cross-section than to the member. That is why it can be calculated very efficiently by semi-analytical FSM, and that is why it can readily be utilized in design approaches as DSM. But on the other hand, that is why the critical load predicted by the signature curve is sometimes questionable, for example when the loading and/or boundary conditions of the member do not allow the formation of the buckled shape as assumed by the signature curve. Moreover, it is theoretically and practically problematic to generate signature curve for members with non-uniform cross-section, e.g., if significant holes are present.

However, the signature curve can be interpreted and constructed in a slightly different way, too, even if keeping the limits of semi-analytical FSM. The alternative way is to fix the length of the (globally and locally hinged) prismatic member, but systematically changing the number of half-waves from 1 to an arbitrarily large number. (According to FSM notations: changing the value of m in Eqs. (1)-(3)). This means that the half-wave length (which is essentially the buckling length) takes various values, the largest one being equal to the actual member length, the next one being equal to one-half of the member length, the third one to one-third of the member length, and so on till an arbitrarily small buckling length. In case of FSM this approach leads to exactly the same signature curve, with the only (rather theoretical) difference that for a given member only discrete points of the curve can be calculated.

If signature curve is interpreted in accordance with this latter approach, the notion of signature curve belongs rather to the member than to the cross-section. This approach can easily be generalized, as follows. First, let us assume that we have a thin-walled member, arbitrarily loaded, with or without holes, but locally and globally hinged at its ends. In this case the same longitudinal shape functions can be used as in semi-analytical FSM, and the buckling problem can be solved by forcing the member to buckle in accordance with the sine-cosine longitudinal displacement distributions. If the number of half-waves is systematically changing, and the problem is solved repeatedly, the lowest critical values can be plotted in the function of the half-wave lengths, leading to a curve essentially similar to the classic signature curve.

If arbitrary boundary conditions are to be handled, the trigonometric longitudinal shape functions must be extended by adding extra shape functions. This requires some further considerations, and these cases are not discussed here.

To construct the generalized signature curves, therefore, we need a numerical method that can solve arbitrary thin-walled member problems, but we need to be able to ensure the required specific trigonometric shape functions. The most obvious general numerical method to use is shell finite element method, and the specific longitudinal shape functions are implemented into the recently proposed constrained finite element method.

4. Signature curves by cFEM for a uniform, compressed column

First a simply supported uniformly compressed column problem is solved. The cross-section is C-shaped, with 100 mm web depth, 60 mm flange width, 8 mm lip length and 2 mm thickness. (Note, dimensions are mid-line dimensions.) The material is isotropic steel, with 210 GPa Young's modulus and 0.3 Poisson's ratio.

Buckling loads are plotted as a function of buckling half-wave length in Fig. 6, including the classic 'all-mode' signature curve calculated without any constraint for the cross-section deformations, as well as various single-mode curves, i.e., when the cross-section deformations are constrained to have flexural (minor-axis) buckling (F), flexural-torsional buckling (FT), distortional buckling with symmetric cross-section deformations (D-sym) and point-symmetric cross-section deformations (D-point), and local-plate buckling (L). Though the critical load values are determined in various options, (see below,) the differences between the various options are small, hence the curves look very similar.

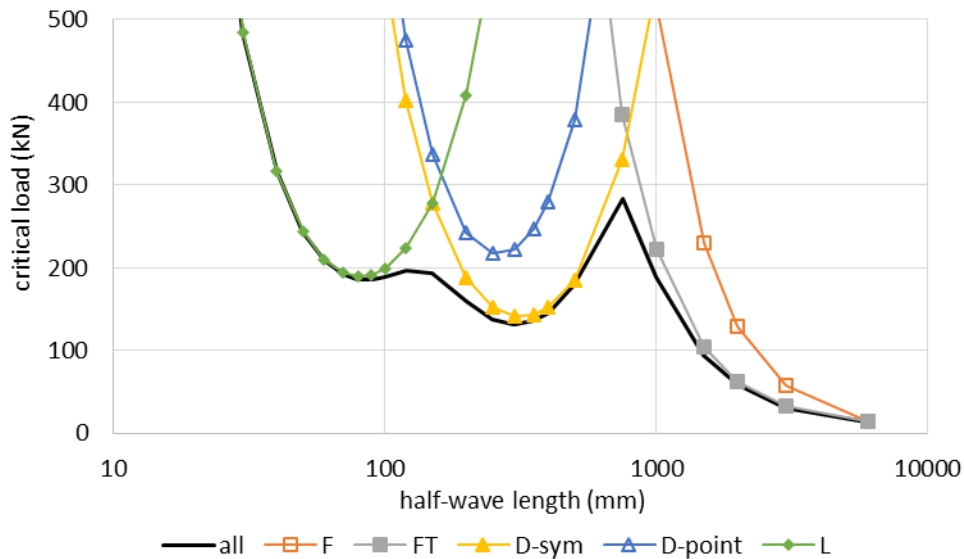


Figure 6: Signature curves for uniform column problem

The calculated critical forces are shown in Table 1 for selected half-wave lengths, including short and long ones, too. The calculations are done in various ways. 'CUFSM' values are calculated by the CUFSM program, using the semi-analytical finite strip method. The other 4 values are calculated by cFEM as follows.

'cFEM 1' is the closest imitation of the FSM. The length of the member is varying while considering one single half-wave. The load is uniform compression, practically no supports are applied (in order not to disturb the uniform stress distribution along the member). Only those second-order strain terms are considered that are associated with the longitudinal normal strain (i.e., the first row of the Green-Lagrange strain vector for 2D strains), identically to how second-order strains are handled in CUFSM. As the results show, 'CUFSM' and 'cFEM 1' values are practically identical, the small differences are caused mostly by the differences in cross-section discretization.

‘cFEM 2’ is similar to ‘cFEM 1’, but all the second-order strain terms are considered from the Green-Lagrange strain vector. Moreover, hinged end supports are defined (by restricting out-of-plane translations of all the FE nodes at both end sections of the member), which results in disturbed stress distribution near to member ends. This disturbed stress distribution has negligible effect for longer members, but causes 2-3% difference for short members.

‘cFEM 3’ follows the concept of generalized signature curve. Each value is calculated on the same FE model: 6000-mm-long column with hinged supports (realized by restricting out-of-plane translations of all the FE nodes at both end sections of the member). All the second-order strain terms are considered, as usual in a general purpose FE calculation. The half-wave length is systematically changed in order to get the values of the generalized signature curve. In this case a moderately dense cross-section discretization is used with approx. 10 mm element width. The longitudinal discretization is relatively coarse, with approx. 27 mm element length. This means that the results are numerically imprecise if the half-wave length is smaller than approx. 50-80 mm, since in these cases one half-wave should be approximated by less than 2-3 cubic polynomials.

‘cFEM 4’ is similar to ‘cFEM 3’, but with a much finer discretization, the width and length of the finite elements being around 5 mm and 9 mm, respectively. This discretization is dense enough to yield to numerically precise results even for half-wave-lengths down to 20-30 mm. As the values of Table 1 prove, ‘cFEM 3’ and ‘cFEM 4’ results are extremely close to the classic ‘CUFSM’ signature curve values.

Table 1: Compressed column: critical forces for selected half-wave lengths

	length mm	all kN	F kN	FT kN	D-sym kN	D-point kN	L kN
CUFSM	30	483.58	91592	74507	5484.9	6309.4	484.08
cFEM 1	30	483.43	91601	74518	5485.2	6309.9	484.02
cFEM 2	30	475.94	91115	74043	5500.1	6344.7	476.50
cFEM 3	30	510.34	93032	76888	6037.0	6941.9	510.87
cFEM 4	30	483.65	91614	74556	5493.1	6319.2	484.22
CUFSM	80	186.75	46397	25394	840.74	976.70	190.13
cFEM 1	80	186.58	46398	25395	840.76	976.75	190.10
cFEM 2	80	180.60	45607	25059	842.53	982.91	183.83
cFEM 3	80	186.61	46452	25439	842.76	979.12	190.08
cFEM 4	80	186.50	46386	25390	840.75	976.78	190.01
CUFSM	300	133.21	5458.3	2313.4	141.55	222.18	793.15
cFEM 1	300	132.05	5458.2	2313.4	141.54	222.15	793.00
cFEM 2	300	132.31	5406.4	2300.3	141.83	222.75	797.70
cFEM 3	300	132.10	5455.3	2312.6	141.57	222.21	793.43
cFEM 4	300	132.07	5455.8	2312.7	141.57	222.20	793.32
CUFSM	1000	189.73	514.71	221.49	546.65	1294.1	7880.8
cFEM 1	1000	189.41	514.71	221.49	546.62	1294.0	7879.9
cFEM 2	1000	189.13	513.03	221.09	547.11	1295.2	7922.4
cFEM 3	1000	189.53	514.42	221.43	546.74	1294.3	7888.6
cFEM 4	1000	189.25	514.47	221.45	546.72	1294.3	7886.7
CUFSM	6000	13.086	14.363	14.879	18122	44836	280605
cFEM 1	6000	13.076	14.363	14.879	18122	44835	280613
cFEM 2	6000	13.069	14.355	14.873	18125	44843	280909
cFEM 3	6000	13.069	14.355	14.873	18125	44843	280909
cFEM 4	6000	13.059	14.356	14.874	18125	44842	280835

5. Signature curves by cFEM for non-uniform problems

Let us consider a member similar to the one discussed in the previous Section, but now it is a beam loaded by uniformly distributed transverse load. The load is acting upward, either at the junction of the upper flange and the web ('Load1'), or on the flange 10 mm apart from the web-to-flange junction ('Load2'). The upper (i.e., tensioned) flange might be laterally free ('Free'), or elastically supported ('Spring') by a weak distributed spring (10 N/mm/mm). As a reference, signature curve for a beam in uniform bending is also calculated by CUFSM.

Fig. 7 shows 'all-mode' signature curves for three cases: classic signature curve for beam ('CUFSM'), generalized signature curve for 'Load1-Free' option, and generalized signature curve for 'Load2-Spring' option. It is important to observe that all the three curves are similar, all having two minimum points at smaller lengths. The buckling loads, however, are dependent on the loading and support. As expected, the critical load values are significantly higher (compared to classic CUFSM case) if the real stress distribution is considered. The applied (though weak) lateral elastic spring support has significant effect on the signature curve, too, especially for medium half-wave lengths. More information can be gained by looking at the numerical values, as discussed below.

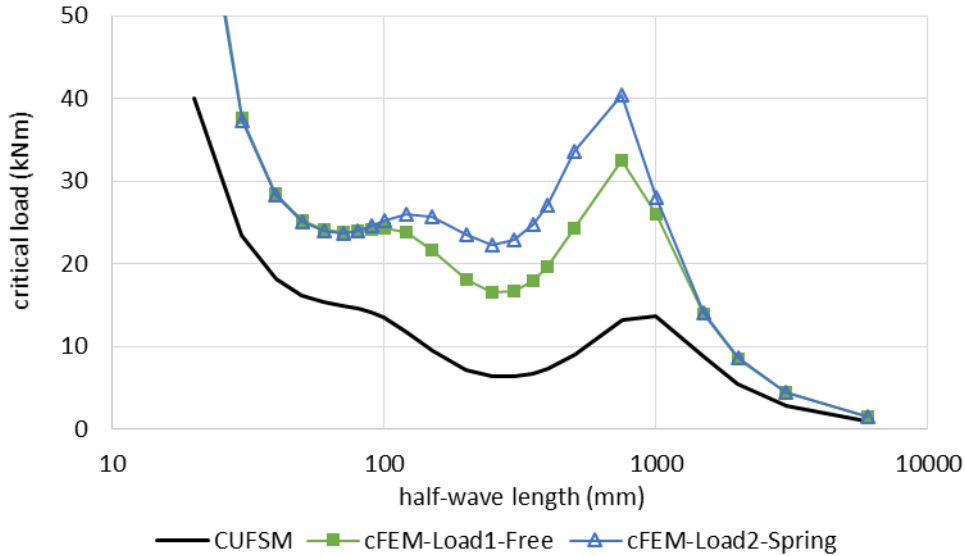


Figure 7: Generalized signature curves for selected beam problems

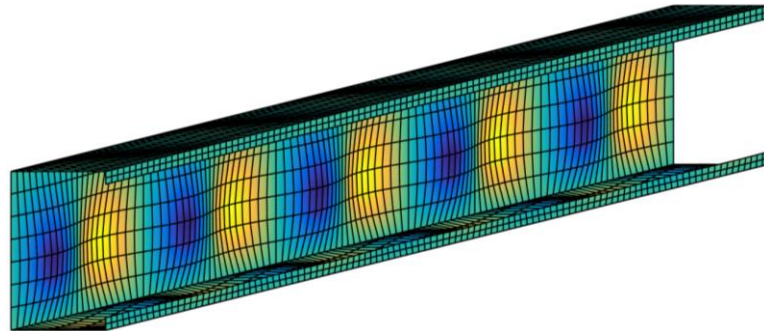
Table 2 shows the calculated critical moments for selected half-wave lengths, including the lengths close to the local minimum (80 mm) and distortional minimum (300 mm). In the table the 'all-mode' critical moment values, as well as pure G, pure D, and pure L values are given. According to the numerical values of Table 2, the distortional critical loads are roughly tripled in case of UDL compared to uniform bending (see 'CUFSM' vs. 'cFEM-Load1-Free' values), but also the global and local critical loads are significantly increased. The lateral support for the upper flange (together with the increased load eccentricity) further increases the critical load values in case of global and, especially, distortional buckling (see 'cFEM-Load1-Free' vs. 'cFEM-Load2-Spring' values), but slightly decreases the critical loads in case of local buckling. The actual numerical values in the last, 'cFEM-Load2-Spring' option are the resultants of various factors, most importantly: the complicated stress distribution (from global bending and torsion, and from the direct transverse bending of the upper flange), the load introduction point (i.e., upper flange, which has an

stabilizing effect on the global and distortional behavior), and the elastic support for the upper flange (which influences the stress distribution, plus seriously affects the possible deformations).

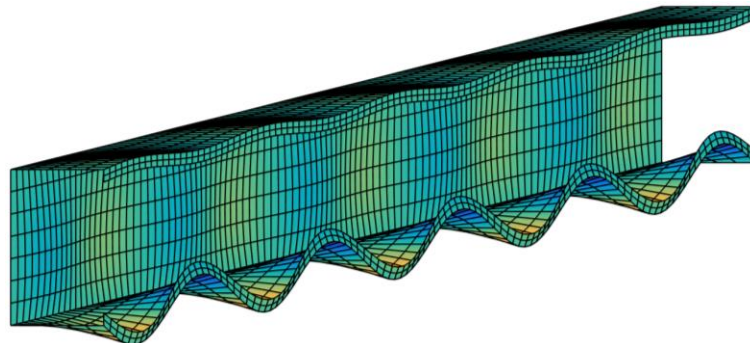
Table 2: Beam problems: critical moments for selected half-wave lengths

	length mm	all kNm	G kNm	D kNm	L kNm
CUFSM	80	14.62	2003.6	34.43	18.86
cFEM-Load1-Free	80	23.92	3415	96.12	27.43
cFEM-Load2-Spring	80	20.12	4989	1072.41	20.64
CUFSM	300	6.308	239.70	6.736	108.81
cFEM-Load1-Free	300	16.69	364.71	18.82	139.38
cFEM-Load2-Spring	300	47.94	512.4	246.97	94.04
CUFSM	1000	13.62	23.13	31.95	1107.3
cFEM-Load1-Free	1000	25.99	35.11	96.64	592.2
cFEM-Load2-Spring	1000	35.96	49.47	→ inf	450.5
CUFSM	3000	2.788	3.042	271.97	9886.3
cFEM-Load1-Free	3000	4.382	4.849	3494.7	722.0
cFEM-Load2-Spring	3000	6.441	7.394	→ inf	573.3

It is to underline that, according to the concept of the proposed generalized signature curve, in all these cases the buckling shape is highly regular, consisting of equal amplitude sinusoidal displacements along the length, even if the loading is non-uniform. (This is illustrated in Fig. 8, where some buckled shapes are shown.) Thus, the critical loads of the generalized signature curves are higher than the ones that would be predicted by an ordinary (shell FE) linear buckling analysis.



'Load2-Spring', 10 half-waves (half.wave length is 600 mm), local plate buckling



'Load1-Free', 10 half-waves (half.wave length is 600 mm), distortional buckling

Figure 8: Buckled shape samples of generalized signature curves for beam problems

6. Signature curves by cFEM for members with holes

In this Section the column problem is studied that presented in Section 4, however, holes are considered in the member. Results are shown here for three hole patterns, see Table 3, compared to the case without holes (identified as ‘NoHole’, which case is identical to the option ‘cFEM 3’ of Section 4). If holes are present, they are rectangular and located in the web.

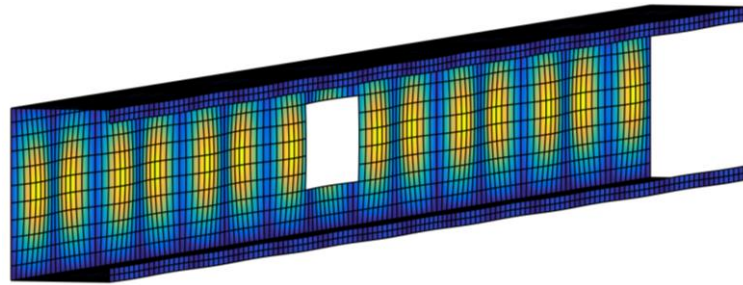
In the first case (‘Hole1’) one centrally placed hole row is considered, the hole dimensions are 50 and 30 mm in the longitudinal and transverse direction, respectively, while the period of the holes is 100 mm (longitudinally), meaning that the distance between two neighboring holes is 50 mm. The second hole pattern is consisted of a few but larger size holes, namely: hole dimensions are 100 and 50 mm in the longitudinal and transverse direction, respectively, while the period of the holes is 1000 mm (longitudinally), meaning that there are only 6 holes in the 6-m-long member. In the third case (‘Hole3’) there are many smaller holes, arranged in 4 rows. The hole dimensions are 20 and 10 mm in the longitudinal and transverse direction, respectively, while the period of the holes is 40 mm and 20 mm, in the longitudinal and transverse direction, respectively.

The calculated critical forces are summarized in Table 3 for selected wave-lengths. Some buckled shapes are illustrated in Fig. 9, however, for the sake of better visibility the deformations are shown on a shorter (1200-mm-long) member.

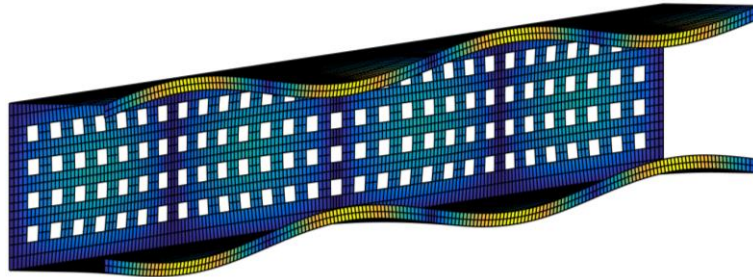
As the numerical values in Table 3 shows, the introduction of web openings can decrease or increase the critical load, depending on the half-wave length (or, depending on which type of buckling is dominant for a given half-wave length) and on the hole pattern. The effect of holes is a resultant of two major factors. One is that the holes (significantly) disturbs the uniform stress distribution, obviously determined by the loading and the hole pattern. The other major factor is that the holes reduces the stiffness. This reduction is greatly dependent on the hole pattern and on the given stiffness (e.g., overall minor-axis flexural stiffness, or overall torsional stiffness, or plate bending stiffness, etc.).

Table 3: Compressed column with holes: critical forces for selected half-wave lengths

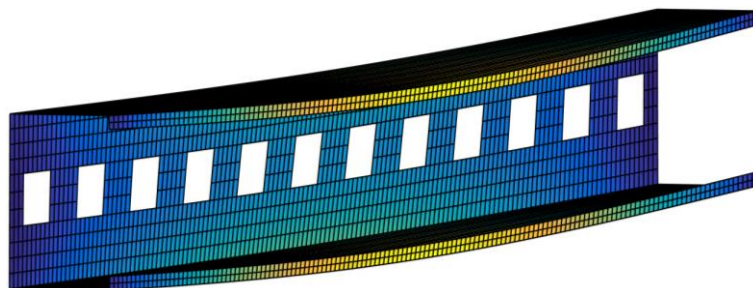
	length mm	all kN	F kN	FT kN	D-sym kN	D-point kN	L kN
cFEM-NoHole	80	186.61	46452	25439	842.76	979.12	190.08
cFEM-Hole1	80	231.92	45047	24181	890.51	1014.6	240.83
cFEM-Hole2	80	199.77	46083	24897	861.32	994.59	204.26
cFEM-Hole3	80	181.78	44507	23463	886.99	1024.7	185.45
cFEM-NoHole	300	132.10	5455.3	2312.6	141.57	222.21	793.43
cFEM-Hole1	300	129.61	5199.2	2237.4	144.67	230.26	972.89
cFEM-Hole2	300	132.71	5371.3	2276.9	143.05	225.40	849.26
cFEM-Hole3	300	124.93	5112.9	2156.9	142.29	227.90	801.86
cFEM-NoHole	1000	189.53	514.42	221.43	546.74	1294.3	7888.6
cFEM-Hole1	1000	183.88	489.21	214.08	530.15	1389.5	7815.3
cFEM-Hole2	1000	187.47	497.73	218.91	534.47	1340.9	9640.2
cFEM-Hole3	1000	177.05	480.78	206.43	513.80	1356.5	7559.5
cFEM-NoHole	6000	13.069	14.355	14.873	18125	44843	280909
cFEM-Hole1	6000	12.384	13.649	14.076	33826	→ inf	22433
cFEM-Hole2	6000	12.850	14.120	14.333	21553	→ inf	80246
cFEM-Hole3	6000	12.133	13.412	13.837	76260	→ inf	37125



'Hole2', 15 half-waves (half.wave length is 80 mm), local plate buckling



'Hole3', 4 half-waves (half.wave length is 300 mm), symmetric distortional buckling



'Hole1', 1 half-wave (half.wave length is 1200 mm), flexural-torsional buckling

Figure 9: Buckled shape samples of generalized signature curves for columns with holes

7. Concluding remarks

In this paper the generalization of the concept of signature curve is presented. To calculate the generalized signature curves a numerical method is necessary that can solve thin-walled member problems, and is able to ensure specific trigonometric displacement distributions in the longitudinal direction. The recently proposed constrained finite element method has all these necessary capabilities, hence it was used to solve proof-of-concept problems. Based on the presented examples it can be concluded that for simple cases the generalized signature curves are practically identical to the classic signature curves. It is also proved, however, that generalized signature curves can be calculated for various non-uniform members.

Though classic signature curves are widely used in the design of cold-formed steel members, it is an open question whether the generalized signature curves can directly be used in design. Nevertheless, it is believed that they help in understanding the complex stability behavior of thin-walled members. While modal decomposition is a useful tool in describing and analyzing the cross-section deformations, the concept of generalized signature curve can contribute to understand the buckling behavior longitudinally, especially for non-uniform problems.

Acknowledgments

The presented work was conducted with the financial support of the K119440 project of the National Research, Development and Innovation Office of Hungary.

References

- Ádány, S., Schafer, B.W. (2006a). Buckling mode decomposition of single-branched open cross-section members via Finite Strip Method: derivation, *Thin-Walled Structures* **44**(5), pp. 563-584.
- Ádány, S., Schafer, B.W. (2006b). Buckling mode decomposition of single-branched open cross-section members via Finite Strip Method: application and examples, *Thin-Walled Structures*, **44**(5), pp. 585-600.
- Ádány S., Schafer B.W. (2014a), Generalized constrained finite strip method for thin-walled members with arbitrary cross-section: Primary modes, *Thin-Walled Structures*, Vol 84, pp. 150-169. 2014.
- Ádány S., Schafer B.W. (2014b), Generalized constrained finite strip method for thin-walled members with arbitrary cross-section: Secondary modes, orthogonality, examples, *Thin-Walled Structures*, Vol 84, pp. 123-133. 2014.
- Ádány S. (2016a), Shell element for constrained finite element analysis of thin-walled structural members, *Thin-Walled Structures*, Volume 105, August 2016, Pages 135-146.
- Ádány S. (2016b), Constrained finite element method for the analysis of shear buckling of thin-walled members, In: Ben Young, Yancheng Cai (szerk.) *Proceedings of the 8th International Conference on Steel and Aluminium Structures*. Hong Kong: University of Hong Kong, 2016. pp. 1-18, 2016.
- Ádány S. (2017a), Constrained shell Finite Element Method for thin-walled members, Part1: constraints for a single band of finite elements, *Thin-Walled Structures*, 2017. doi:10.1016/j.tws.2017.01.015
- Ádány S. (2017b), Constrained shell Finite Element Method for thin-walled members with holes, *Thin-Walled Structures*, vol 121, pp. 41-56. (2017)
- Ádány S. (2017c), Non-uniform modal decomposition of thin-walled members by the constrained finite element method, *Proceedings of the Annual Stability Conference*, San Antonio, USA, 2017.03.21-2017.03.24. Structural Stability Research Council, pp. 1-16, Paper #52, 2017.
- Ádány S, Visy D, Nagy R (2017), Constrained shell Finite Element Method, Part 2: application to linear buckling analysis of thin-walled members, *Thin-Walled Structures*, 2017. doi:10.1016/j.tws.2017.01.022
- Bebiano R., Gonçalves R., Camotim D. (2015), A cross-section analysis procedure to rationalise and automate the performance of GBT-based structural analyses, *Thin-Walled Structures*, Vol 92, pp. 29-47, 2015.
- Cheung, Y.K. (1976). Finite strip method in structural analysis, Pergamon Press, 1976.
- CUFSM (2006), Elastic buckling analysis of thin-walled members by finite strip analysis. CUFSM 2006; v3.12. <http://www.ce.jhu.edu/bschafer/cufsm>.
- DSM (2006), American Iron and Steel Institute. Direct strength method design guide. Washington, DC, USA; 2006
- Hancock, G.J. (1978), Local, Distortional, and lateral buckling of I-beams, *ASCE Journal of structural engineering*, 104(11), pp. 1787-1798.
- Hoang T, Ádány S (2017), On the use of constrained finite element method in the design of cold-formed steel Z purlins, *Proceedings of the Eurosteel 2017 conference*, Sept 13–15, 2017, Copenhagen, Denmark. Ernst & Sohn Verlag für Architektur und technische Wissenschaften GmbH & Co. KG, Berlin, CE/papers (2017)
- Pham C.H., Hancock G.J. (2013), Shear buckling of channels using the semi-analytical and spline finite strip methods. *Journal of Constructional Steel Research*, 90, pp. 42-48, 2013.
- THIN-WALL (1995), School of Civil Engineering, University of Sydney, Sydney, Australia, 1995.
- Silvestre N., Camotim D., Silva N.F. (2011), Generalized Beam Theory revisited: from the kinematical assumptions to the deformation mode determination, *Int. Journal of Structural Stability and Dynamics*, 11(5), pp. 969-997, 2011.
- Visy D, Ádány S (2017), Local Elastic and Geometric Stiffness Matrices for the Shell Element Applied in cFEM, *Periodica Polytechnica ser. Civil Engineering*, 61(3), pp. 569-580, 2017.